572767

NASA/TM—2002-211364

Vacuum Ultraviolet Radiation and Atomic Oxygen Durability Evaluation of HST Bi-Stem Thermal Shield Materials

Joyce Dever and Kim K. de Groh
Glenn Research Center, Cleveland, Ohio

February 2002

The NASA STI Program Office . . . in Profile

Since its founding, NASA has been dedicated to the advancement of aeronautics and space science. The NASA Scientific and Technical Information (STI) Program Office plays a key part in helping NASA maintain this important role.

The NASA STI Program Office is operated by Langley Research Center, the Lead Center for NASA's scientific and technical information. The NASA STI Program Office provides access to the NASA STI Database, the largest collection of aeronautical and space science STI in the world. The Program Office is also NASA's institutional mechanism for disseminating the results of its research and development activities. These results are published by NASA in the NASA STI Report Series, which includes the following report types:

- TECHNICAL PUBLICATION. Reports of completed research or a major significant phase of research that present the results of NASA programs and include extensive data or theoretical analysis. Includes compilations of significant scientific and technical data and information deemed to be of continuing reference value. NASA's counterpart of peer-reviewed formal professional papers but has less stringent limitations on manuscript length and extent of graphic presentations.

- TECHNICAL MEMORANDUM. Scientific and technical findings that are preliminary or of specialized interest, e.g., quick release reports, working papers, and bibliographies that contain minimal annotation. Does not contain extensive analysis.

- CONTRACTOR REPORT. Scientific and technical findings by NASA-sponsored contractors and grantees.

- CONFERENCE PUBLICATION. Collected papers from scientific and technical conferences, symposia, seminars, or other meetings sponsored or cosponsored by NASA.

- SPECIAL PUBLICATION. Scientific, technical, or historical information from NASA programs, projects, and missions, often concerned with subjects having substantial public interest.

- TECHNICAL TRANSLATION. English-language translations of foreign scientific and technical material pertinent to NASA's mission.

Specialized services that complement the STI Program Office's diverse offerings include creating custom thesauri, building customized data bases, organizing and publishing research results . . . even providing videos.

For more information about the NASA STI Program Office, see the following:

- Access the NASA STI Program Home Page at ***http://www.sti.nasa.gov***

- E-mail your question via the Internet to help@sti.nasa.gov

- Fax your question to the NASA Access Help Desk at 301–621–0134

- Telephone the NASA Access Help Desk at 301–621–0390

- Write to:
  NASA Access Help Desk
  NASA Center for AeroSpace Information
  7121 Standard Drive
  Hanover, MD 21076

NASA/TM—2002-211364

Vacuum Ultraviolet Radiation and Atomic Oxygen Durability Evaluation of HST Bi-Stem Thermal Shield Materials

Joyce Dever and Kim K. de Groh
Glenn Research Center, Cleveland, Ohio

National Aeronautics and
Space Administration

Glenn Research Center

February 2002

Acknowledgments

The authors would like to acknowledge the technical contributions of the following: Bruce Banks and Sharon Miller of the NASA GRC Electro-Physics Branch, Curtis Stidham and Thomas Stueber of the NYMA, Inc., SETAR Team, Deborah Hotes of CWRU, Anthony Pietromica of the Ohio Aerospace Institute, Charles Pennington and Michael Woidke of the NASA GRC Test Installations Division, Marvin Smith of InDyne, Inc., Tim McCollum and Cara McCracken of Cleveland State University, Mervin Bridges of NIST, Kevin Kjoller of Digital Instruments, Edward Gaddy and Greg Greer of NASA GSFC, Ralph Sullivan and Chris Hoffman of Swales and Associates, and Thomas Zuby and Aaron Pokrass of Unisys.

Trade names or manufacturers' names are used in this report for identification only. This usage does not constitute an official endorsement, either expressed or implied, by the National Aeronautics and Space Administration.

Available from

NASA Center for Aerospace Information
7121 Standard Drive
Hanover, MD 21076

National Technical Information Service
5285 Port Royal Road
Springfield, VA 22100

Available electronically at http://gltrs.grc.nasa.gov/GLTRS

VACUUM ULTRAVIOLET RADIATION AND ATOMIC OXYGEN DURABILITY EVALUATION OF HST BI-STEM THERMAL SHIELD MATERIALS

Joyce A. Dever and Kim K. de Groh
National Aeronautics and Space Administration
Glenn Research Center
Cleveland, Ohio 44135

ABSTRACT

Bellows-type thermal shields were used on the bi-stems of replacement solar arrays installed on the Hubble Space Telescope (HST) during the first HST servicing mission (SM1) in December 1993. These thermal shields helped reduce the problem of thermal gradient-induced jitter observed with the original HST solar arrays during orbital thermal cycling and have been in use on HST for eight years. This paper describes atomic oxygen (AO) and combined AO and vacuum ultraviolet (VUV) radiation ground testing of the candidate solar array bi-stem thermal shield materials including backside aluminized Teflon® FEP (fluorinated ethylene propylene) with and without AO and ultraviolet radiation protective surface coatings. NASA Glenn Research Center (GRC) conducted VUV and AO exposures of samples of candidate thermal shield materials at HST operational temperatures and pre- and post-exposure analyses as part of an overall program coordinated by NASA Goddard Space Flight Center (GSFC) to determine the on-orbit durability of these materials.

Coating adhesion problems were observed for samples having the AO- and combined AO/UV-protective coatings. Coating delamination occurred with rapid thermal cycling testing which simulated orbital thermal cycling. This lack of adhesion caused production of coating flakes from the material that would have posed a serious risk to HST optics if the coated materials were used for the bi-stem thermal shields. No serious degradation was observed for the uncoated aluminized Teflon® as evaluated by optical microscopy, although atomic force microscopy (AFM) microhardness testing revealed that an embrittled surface layer formed on the uncoated Teflon® surface due to vacuum ultraviolet radiation exposure. This embrittled layer was not completely removed by AO erosion. No cracks or particle flakes were produced for the embrittled uncoated material upon exposure to VUV and AO at operational temperatures to an equivalent exposure of approximately five years in the HST environment.

Uncoated aluminized FEP Teflon® was determined to be the most appropriate thermal shield material and was used on the bi-stems of replacement solar arrays installed on HST during SM1 in December 1993. The SM1-installed solar arrays are scheduled to be replaced during HST's fourth servicing mission (SM3B) in early 2002.

1. INTRODUCTION

The Hubble Space Telescope was deployed in low Earth orbit (LEO) on April 25, 1990. Due to thermal gradient-induced jitter observed when the spacecraft passed between sunlight and shadow, bellows-type thermal shields were proposed and used for the bi-stems of the replacement solar arrays installed during the first HST servicing mission (SM1) conducted in December 1993. The locations of the solar array bi-stem thermal shields are indicated in an on-orbit photograph of HST in Figure 1. Figure 2 is a close up view of a segment one of these thermal shields prior to placement on HST showing the bellows structure.

Candidate thermal shield materials were backside aluminized Teflon® FEP (fluorinated ethylene propylene) with and without front surface coatings to protect FEP from atomic oxygen (AO) and combined AO and ultraviolet (UV) radiation. Teflon® FEP, commonly used as a thermal control material, is known to be susceptible to damage by atomic oxygen and ultraviolet radiation. Atomic oxygen causes erosion of polymer materials [Ref. 1], and ultraviolet radiation can cause embrittlement of Teflon® [Ref. 2]. Furthermore, since the time of SM1, it has been observed for HST FEP surfaces that thermal cycling and deep layer damage from electrons and protons caused embrittlement and crack propagation at stress concentrations in FEP surfaces and that the extent of FEP damage increased with combined total dose of electron, proton, ultraviolet and x-ray radiation [Ref. 3].

Ground laboratory evaluation of the candidate aluminized Teflon® FEP thermal shield materials was conducted to determine which material(s) would be appropriate for a lifetime of approximately 5 years in the HST environment, the anticipated lifetime of the SM1 replacement solar arrays. The overall plan for ground laboratory durability testing was developed by GSFC with input from GRC and called for sequential exposure of candidate materials to electron radiation, rapid thermal cycling (RTC), VUV, and combined AO/VUV exposures at operational temperatures. Although protons and solar flare x-rays are also part of the HST orbital environment, evaluation of their effects was not included in this testing. This report summarizes GRC's contributions to the testing of the thermal shields for the HST SM1 replacement solar arrays installed in December 1993. GRC evaluated the effects

of VUV and combined AO/VUV exposure at HST operational temperatures. Analyses conducted by GRC included optical microscopy and surface microhardness characterization. GRC evaluated the condition of the surfaces of all samples prior to and after conducting VUV and AO/VUV exposures. GRC also evaluated whether an embrittled layer would build up on the uncoated aluminized FEP Teflon® due to five-year orbital equivalent exposures of VUV and AO. Following the GRC exposures, representative samples were returned to GSFC for additional analysis.

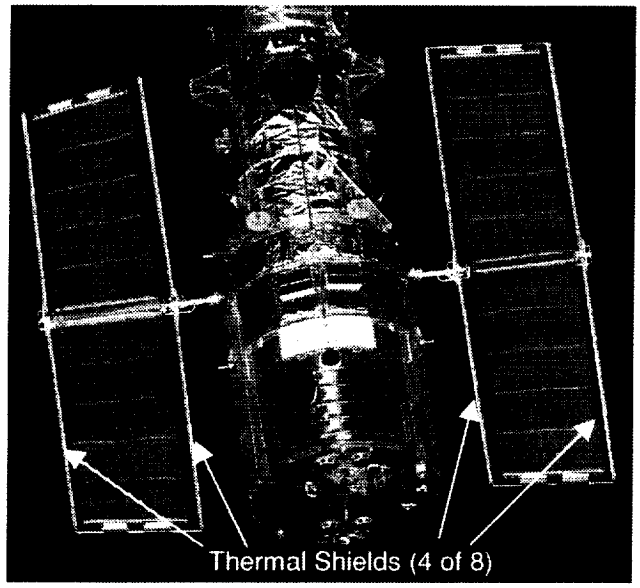

Figure 1: On-orbit view of the Hubble Space Telescope indicating positions of the 8 solar array bi-stem thermal shields.

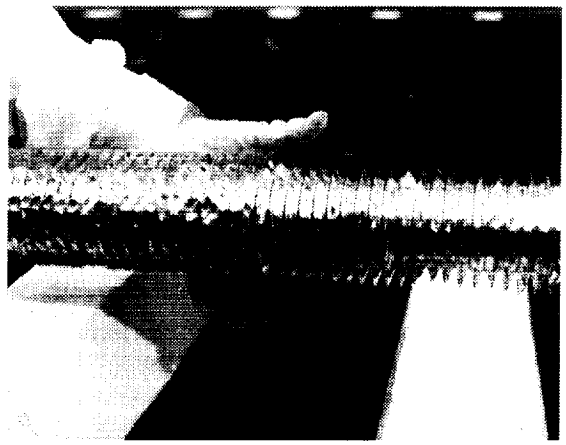

Figure 2: Close up view of aluminized Teflon® FEP bellows structure of bi-stem thermal shield [Ref. 4].

2. EXPERIMENTAL

2.1 Description of Samples

To form the thermal shields, rings of backside aluminized Teflon® FEP were thermally fused (welded) together to form a bellows assembly. The basic uncoated aluminized FEP material was comprised of 0.002" (50.8 μm) thick Teflon® FEP with vapor deposited aluminum of 1000 Å nominal thickness on the backside. The bellows assemblies, a section of which is shown in Figure 2, were fabricated by Sheldahl, Inc. and supplied to GSFC through the European Space Agency, the suppliers of the HST SM1-installed solar arrays. The prime candidate material for the HST solar array bi-stem thermal shields was the backside aluminized FEP with alternating layers of SiO_2, TiO_2, and Ta_2O_3 deposited on the front, or space-facing FEP surface. This coating was developed and deposited by Optical Coating Laboratory, Inc. (OCLI) and is referred to as OCLI/FEP/Al. This coating was optimized to protect the underlying FEP Teflon® from UV radiation absorption and is also atomic oxygen

protective. A second candidate material was backside aluminized FEP with an atomic oxygen protective surface coating of SiO_X deposited by GSFC referred to as SiO_X/FEP/Al. Deposition of the OCLI and SiO_X coatings onto the bellows thermal shields was done in sections, because of the small size of the deposition chambers with respect to the size of a deployed thermal shield. Overlap areas were necessary at adjoining coated sections to assure complete coverage. These overlap areas were "double-coated," receiving double the thickness of a single layer. Therefore, both single- and double-coated SiO_X- and OCLI-coated samples were evaluated in the environmental durability testing. A single layer of SiO_X coating may have been as thick as 1600 Å, and a single layer of the OCLI coating varied from approximately 3500 Å to 7000 Å. The third candidate thermal shield material was the backside aluminized FEP (FEP/Al) with no front surface coating.

Two types of sample configurations for the thermal shield materials were tested at GRC: planar (flat) samples and welded (bellows section) samples. The planar samples were cut either from bellows sections or, in the case of uncoated samples, from aluminized FEP sheet stock. Sample holders were constructed to hold planar samples at the same angle that the surfaces of the welded samples would be with respect to the VUV source or to the AO-VUV beam in the various tests (approximately 23.5° from normal). This was done to simulate the solar exposure angle that would be received by the bellows surfaces on orbit. Three groups of samples designated as Sample Groups 1, 2 and 3 contained the various types of candidate thermal shield materials for VUV and AO-VUV exposure. Samples were tested in three groups because there were three compartments for VUV exposure. Sample labels for the thermal shield candidates used the following configuration: "prefix-sample number." The prefix designations are described in Table 1 indicating the type of sample, type of surface coating, and, if coated, whether the sample was single- or double-coated. During the course of testing, some samples were replaced with new ones because of improvements in coating processes or because of sample failures. Samples in the original set have sample numbers ranging from "-01" to "-11", whereas replacement samples have sample numbers ranging from "-101" to "-108" and "-201" to "-210." By the conclusion of VUV and AO exposure testing at GRC, there were 79 candidate thermal shield samples, which received various levels of exposure to VUV and AO. A photograph of one of the three sample groups is shown in Figure 3 indicating planar and welded samples. A schematic showing the layout of all three sample groups is shown in Figure 4. When more than one sample label appears in a given location in Figure 4, this indicates that the original sample was replaced at some point during the test.

In addition to the candidate thermal shield samples, each sample group also included a planar sample of backside aluminized FEP with a thermocouple attached to the back with aluminized FEP tape. For each sample group, this temperature monitor sample is referred to as "TMP." Each sample group also included two contamination witness mirrors (Ctm1 and Ctm 2) comprised of glass slides coated with approximately 1000 Å of vapor deposited aluminum followed by 10,000 Å of SiO_X. These were located among the planar samples. The TMP and Ctm samples are indicated in Figure 3. Sample Groups 1 and 2 included a planar silvered Teflon® optical solar reflector, SRa-01 and SRa-02, respectively, for durability comparison to the thermal shield candidates, because much previous data was available for space durability of optical solar reflectors. Finally, each sample group included a fixture for holding uncoated aluminized Teflon® sample strips for atomic force microscopy (AFM) microhardness analysis of the FEP surfaces exposed to various durations of atomic oxygen and VUV. These fixtures were also held at 23.5° from normal, and were positioned between fasteners on the welded sample fixtures. An AFM sample holder can be seen in Figure 3. The AFM samples will be described in more detail in the Analysis Methods section.

TABLE 1 - SAMPLE TYPES

Prefix	Type of Sample
a-	Planar
b-	Welded
ra- or rb-	Single coated, OCLI
rra- or rrb-	Double coated, OCLI
sa- or sb-	Single coated, SiO_X
ssa- or ssb-	Double coated, SiO_X
ua- or ub-	Uncoated aluminized FEP Teflon®
SRa-	Planar silvered Teflon® sample
TMP	Temperature monitor
Ctm1	Contamination monitor
Ctm2	Contamination monitor
AFM	Atomic Force microscopy sample assembly

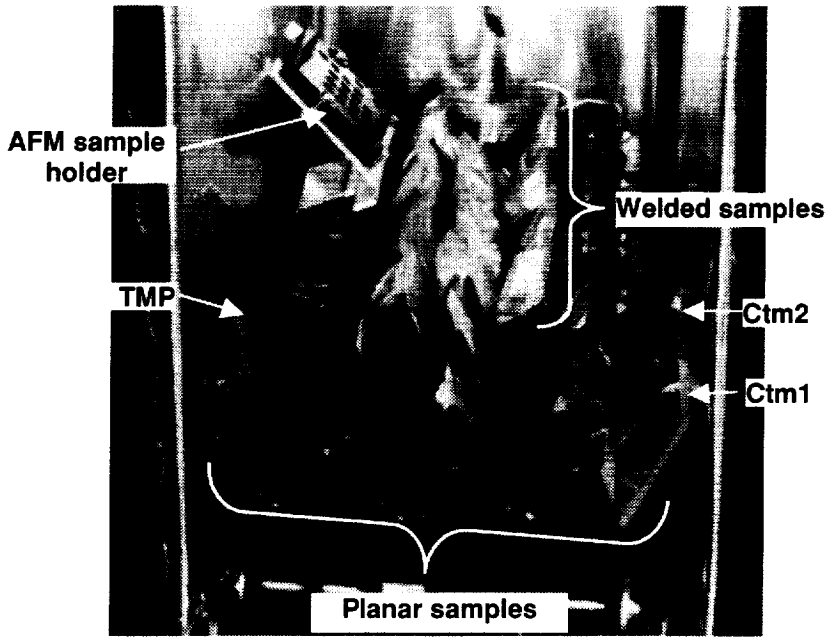

Figure 3: Photograph of one of the three sample groups for VUV and AO-VUV exposure of HST thermal shield candidate materials.

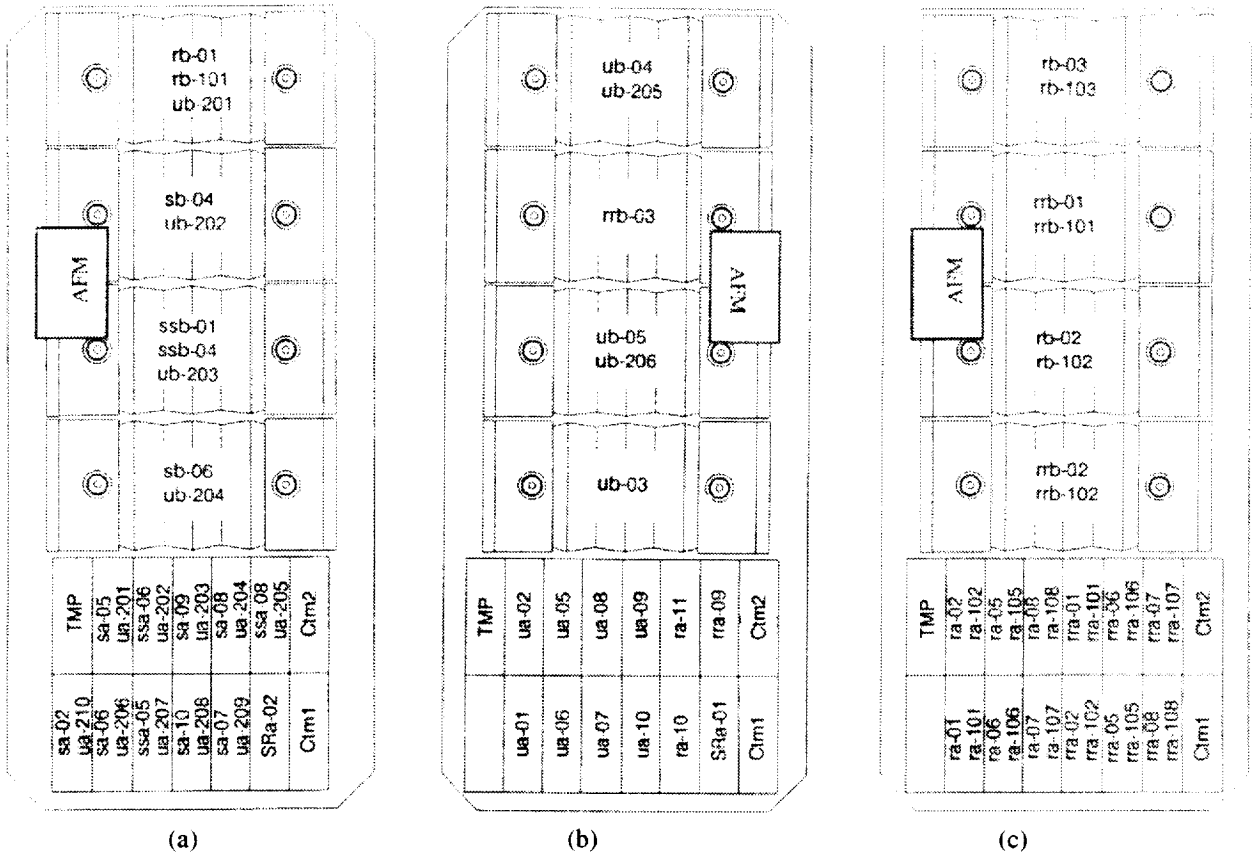

Figure 4: Configuration of samples in holders for (a) Sample Group 1, (b) Sample Group 2, and (c) Sample Group 3.

2.2 Environmental Exposure Testing

Environmental exposure conditions for all thermal shield samples are given in Tables 2A-C including electron radiation, rapid thermal cycling, vacuum ultraviolet equivalent sun hours (ESH) and atomic oxygen fluence.

2.2.1 Sample Treatment Prior To GRC Testing

Prior to being sent to GRC, some planar samples were bent to induce cracks in the aluminum layer prior to further testing by bending around a mandrel 25 times with the FEP side in tension and 25 times with the aluminum side in tension. Many of the samples were then exposed to electron radiation from a Van de Graaf accelerator with an energy of 1 MeV to a calculated absorbed dose of 0.5 Mrads estimated to provide an equivalent of five years in the HST environment. The calculated dose was based on the stopping power of polytetrafluoroethylene (PTFE), chemically very similar to FEP, because data were not available for the stopping power of FEP. Following electron irradiation, some samples were also exposed to 175 rapid thermal cycles (RTC) representative of approximately 11 days on HST. The nominal temperature cycling range expected on HST was –150 to 105 °C for SiO_X-coated and uncoated aluminized FEP and –150 to 135 °C for OCLI-coated aluminized FEP. These were the target temperature ranges for RTC testing. The upper temperature limits were calculated based on optical properties. Due to equipment malfunctions, the RTC testing was not well controlled, and the nominal range of cycling was between –115 and 90 °C. Furthermore, equipment failure resulted in some samples falling into the heating element, and it was required that they be replaced by new ones. Because of time and facility limitations, some of these replacement samples did not undergo electron irradiation or RTC exposure prior to VUV and AO-VUV exposure as indicated in Tables 2A-2C.

The upper temperature limit expected for the thermal shields on HST is within the range of the glass I transition temperature (α relaxation) for FEP which ranges from ≈83 to 150 °C and is dependent on hexafluoropropylene (HFP) content [Ref. 5]. Degradation in mechanical properties has been observed for radiation and space exposed FEP that has been heated to 130 and 200 °C [Refs. 6, 7]. The 135 °C upper expected temperature limit is well below the maximum use temperature for FEP of 205 °C and the temperature range for melting of 250 to 280 °C [Ref. 6].

2.2.2 VUV and AO-VUV Exposure in GRC Facilities

For approximately 5 years of service on HST, it was estimated that the thermal shield materials would be exposed to approximately 30,000 hours of UV and an atomic oxygen fluence of 1.2×10^{20} atoms/cm^2. In order to simulate this in the laboratory, the goal was to expose samples to three increments of the following: four weeks of VUV radiation at 15 times the solar intensity (15 suns) in the 115-180 nm wavelength range totaling approximately 10,000 equivalent sun hour (ESH) followed by exposure to 4×10^{19} atoms/cm^2 effective atomic oxygen fluence in the presence of VUV radiation. This would provide the space-expected ratio of AO fluence to VUV equivalent sun hours, or AO/VUV ratio, of $\approx 4 \times 10^{15}$ atoms/cm^2·ESH. Because of lamp output degradation, it was not possible to maintain 15 suns throughout the exposure. Each 4-week increment of VUV testing provided significantly less than 10,000 ESH, although each AO exposure still provided 4×10^{19} atoms/cm^2 fluence. Therefore, for simulation of 5 years in the HST thermal shield environment, the VUV exposure was deficient in comparison to the AO exposure and the actual AO/VUV ratio for exposed samples was greater than 4×10^{15} atoms/cm^2·ESH. Actual values of VUV ESH varied for samples in each of the three exposure chambers as indicated in Tables 2A-2C.

2.2.2.1 VUV Exposure Facility

The VUV exposure facility used three water cooled copper compartments each equipped with a 30-watt deuterium VUV lamp with a magnesium fluoride (MgF_2) window, two 100-watt short-filament quartz halogen heating lamps and copper/constantan thermocouple-instrumented witness samples. A drawing of one of the test compartments is shown in Figure 5. These compartments were located inside of a cryopumped high vacuum chamber that operated at a pressure of approximately 5×10^{-6} torr. Samples were placed on the 7.62 cm x 15.24 cm (3 in. x 6 in.) mounting platform of each of these compartments as shown.

TABLE 2A - ENVIRONMENTAL EXPOSURE PROFILE FOR HST BI-STEM THERMAL SHIELD SAMPLES (SAMPLE GROUP 1)

Sample ID	Sample Description	Bent to induce cracks	Electron radiation exposed[a]	Rapid Thermal Cycled[b]	ESH VUV (115 - 180 nm)	AO Fluence (atoms/cm^2)
rb-01	Welded, OCLI, single-coated		X	X	< 3274	0
ssb-01	Welded, SiO_X, double-coated		X	X	3274	0
ub-202	Welded, uncoated				< 5898	9.28×10^{19}
ub-201	Welded, uncoated				< 5898	9.28×10^{19}
ub-203	Welded, uncoated				5898	9.28×10^{19}
ub-204	Welded, uncoated				5898	9.28×10^{19}
rb-101	Welded, OCLI, single-coated				< 7840	4.0×10^{19}
ssb-04	Welded, SiO_X, double-coated				7840	4.0×10^{19}
sb-04	Welded, SiOx, single-coated		X		< 11,114	4.0×10^{19}
sb-06	Welded, SiO_X, single-coated		X		11,114	4.0×10^{19}
ua-201 to -210	Planar, uncoated				< 5898	9.28×10^{19}
sa-02, -05 to -10; ssa-05, -06, -08	Planar, SiOx-coated (sa=single-coated; ssa=double-coated)	sa-02 only	X	X	< 11,114	4.0×10^{19}
SRa-02	Planar, optical solar reflector (silvered Teflon®)		X	X	< 17,012	1.33×10^{20}

[a] 1 MeV electron exposure for a total dose of 0.5 Mrads
[b] 175 cycles, nominal range of cycling: –115 °C to 90 °C although temperature range varied.

TABLE 2B - ENVIRONMENTAL EXPOSURE PROFILE FOR HST BI-STEM THERMAL SHIELD SAMPLES (SAMPLE GROUP 2)

Sample ID	Sample Description	Bent to induce cracks	Electron radiation exposed[a]	Rapid Thermal Cycled[b]	ESH VUV (115 - 180 nm)	AO Fluence (atoms/cm^2)
ub-205	Welded, uncoated				< 882	2.5×10^{19}
ub-206	Welded, uncoated				5410	9.28×10^{19}
ub-05[c]	Welded, SiO_X-coated		X		11,647	4.0×10^{19}
ub-04[c]	Welded, SiO_X-coated		X		< 16,175	1.08×10^{20}
rrb-03	Welded, OCLI, double-coated				< 17,057	1.33×10^{20}
ub-03	Welded, uncoated		X	X	17,057	1.33×10^{20}
ua-01, -02, -05 to -10	Planar, uncoated	ua-01 ua-02	X	X	< 17,057	1.33×10^{20}
ra-10, -11 rra-09	Planar, OCLI (ra=single-coated, rra=double-coated)				< 17,057	1.33×10^{20}
SRa-01	Planar, optical solar reflector (silvered Teflon®)		X	X	< 17,057	1.33×10^{20}

[a] 1 MeV electron exposure for a total dose of 0.5 Mrads
[b] 175 cycles, nominal range of cycling: –115 °C to 90 °C although temperature range varied.

TABLE 2C - ENVIRONMENTAL EXPOSURE PROFILE FOR HST BI-STEM THERMAL SHIELD SAMPLES (SAMPLE GROUP 3)

Sample ID	Sample Description	Bent to induce cracking	Electron radiation exposed [a]	Rapid Thermal Cycled [b]	ESH VUV (115 - 180 nm)	AO Fluence (atoms/cm^2)
rb-03	Welded, OCLI, single-coated				< 3600	0
rrb-01	Welded, OCLI, double-coated		X	X	< 3600	0
rb-02	Welded, OCLI, single-coated		X	X	3600	0
rrb-02	Welded, OCLI, double-coated		X	X	3600	0
rb-103	Welded, OCLI, single-coated				< 13,335	1.33×10^{20}
rrb-101	Welded, OCLI, double-coated				< 13,335	1.33×10^{20}
rb-102	Welded, OCLI, single-coated				13,335	1.33×10^{20}
rrb-102	Welded, OCLI, double-coated				13,335	1.33×10^{20}
ra-01, -02, -05 to -08; rra-01, -02, -05 to -08	Planar, OCLI (ra=single-coated, rra=double-coated)	ra-01 ra-02	X	X	< 3600	0
ra-101, -102, -105 to -108 rra-101, -102, -105 to -108	Planar, OCLI (ra=single-coated, rra=double-coated)	rra-01 rra-02			< 13,335	1.33×10^{20}

[a] 1 MeV electron exposure for a total dose of 0.5 Mrads
[b] 175 cycles, nominal range of cycling: –115 °C to 90 °C although temperature range varied.

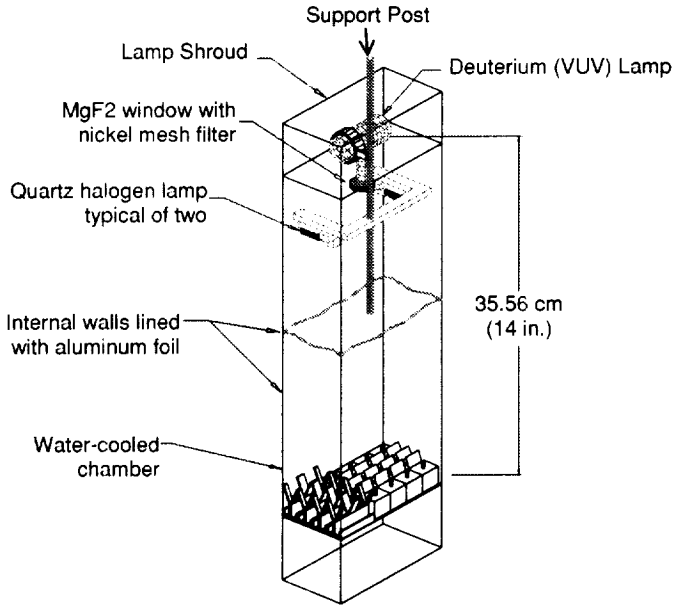

Figure 5: Arrangement of hardware in a typical test chamber in VUV exposure facility.

Lamps used for this testing were assembled with a piece of electroformed nickel mesh of 394 lines/cm (1000 lines/in) in front of their MgF_2 end window. This mesh was used as a neutral density filter to reduce the VUV intensity to the desired level. Because the VUV lamps' MgF_2 end windows were known to darken with

accumulation of VUV-fixed contamination from the facility, it was desired to use an external MgF_2 disk as a sacrificial window that could be replaced with a clean one every 3 to 5 days of running time. It was not expected that the samples would build up contamination in the same way, because the amount of fixed contamination is proportional to VUV intensity, and directly in front of the lamp, VUV intensity was much greater than at the sample site.

Based on the calibration of a representative lamp by the National Institute of Standards and Technology (NIST), it was determined that a typical lamp assembly containing mesh and the additional MgF_2 window could be placed approximately 35.56 cm (14 in.) from the samples to provide 10 to 15 equivalent VUV suns integrated over the wavelength range between 115 and 180 nm, and 3-5 suns in the 115-200 nm range. Transmittance of each sacrificial MgF_2 window was obtained before and after use, and these values were used to calculate the VUV lamp irradiance curve, and thus the pre-exposure and post-exposure intensity for each test increment. Manufacturer-reported intensity degradation with lamp running time was also used in this calculation.

A reasonable intensity distribution (maximum variation of approximately 34%) was calculated for samples within a 5.08 cm (2 in.) diameter exposure area in the middle of the 7.62 cm x 15.24 cm (3 in. x 6 in.) sample area. Equivalent sun hours were calculated based on this center area of the VUV beam. Because the samples filled the chamber, many were outside of the area receiving this reasonable intensity distribution. The maximum variation in intensity over the area of the chamber is approximately 86%, indicating that samples at the back and front of the chambers received approximately 14% of the intensity that samples close to the center received. Tables 2A, 2B and 2C indicate ESH values for samples positioned outside the center illumination area as less than the calculated values for the center area. Details of spectral irradiance and spatial distribution of intensity of the VUV source are described elsewhere [Ref. 8].

Because heating and ultraviolet radiation exposure occur simultaneously for solar-facing HST surfaces, it was important to heat the samples during VUV exposure. A pair of 100-watt short-filament quartz halogen lamps was placed at approximately 30.48 cm (12 in.) above the sample level to either side of the VUV lamp end window in each of the three chambers. For the uncoated and SiO_X-coated samples (Sample Groups 1 and 2, in compartments 1 and 2, respectively), thermocouple temperature in each chamber was maintained at approximately 105 °C, and for the OCLI-coated (Sample Group 3 in compartment 3), thermocouple temperature was maintained at 135°C during VUV exposure. The thermocouple temperature monitor sample provided feedback to a temperature control system that adjusted power to the lamp pairs in each compartment to maintain the programmed temperature. Use of this system ensured the following: (a) temperature of the witness sample would not exceed 3° below or 5° above the desired temperature, (b) temperature data for each witness sample would be recorded to a file and printed out once every minute.

After the first few days of VUV exposure, it was observed that the welded samples were collapsing due to deformation from heating. In order to keep the samples propped up at the appropriate angle, stainless steel wire supports were placed underneath the outer welds for each set of welded samples for the duration of testing.

2.2.2.2 Atomic Oxygen-VUV Exposure Facility

The atomic oxygen-VUV exposure facility used a 1000 watt, 2.45 GHz electron cyclotron resonance (ECR) plasma source to generate a low energy, broad area beam consisting of oxygen atoms, ions, radicals and metastables, where ionic oxygen was estimated to represent <10% of the species present. The neutral oxygen species are at thermal energies, approximately 0.04 to 0.1 eV, and the ions have energies less than 30 eV. Therefore, the energies are not the same as the orbital ram energy of 4.5 eV. However, a correlation can be made between AO erosion produced by the facility and AO erosion which would be produced in space by exposing samples to an "effective" atomic oxygen fluence based on the mass loss of FEP Teflon® whose erosion yield has been determined to be $3.37 \pm 0.05 \times 10^{-25}$ cm^3/atom [Ref. 9]. The arrangement of equipment in the AO-VUV facility is shown in Figure 6. Fused silica fixturing and aluminum foil were used to block unwanted, intense VUV radiation provided by the ECR beam while providing scattered isotropic atomic oxygen arrival at the sample site. A pair of VUV lamps of the type used in the VUV exposure facility (2 of 4 available as shown in Figure 4) was used to provide controlled VUV illumination of the sample area during atomic oxygen exposure. This assured a more uniform VUV intensity distribution across the sample area than could be obtained in the VUV facility. It was assumed that atomic oxygen fluence was uniform and, therefore, identical for all samples. Two quartz halogen lamps rated for up to 100 watts were positioned below the fused silica triangle, approximately 4" above the sample surfaces, and were used to maintain the appropriate temperatures for each sample group using the same temperatures and the same controlling system as was used for VUV exposure. The vacuum system for this facility is comprised of a diffusion pump with a liquid nitrogen trap backed by a Roots-type blower and a rotary vane pump. The pumping system maintains a base vacuum pressure on the order of 10^{-6} torr. The three sample groups were tested one at a time in this facility. Additional details regarding the AO-VUV exposure facility are found elsewhere [Ref. 10].

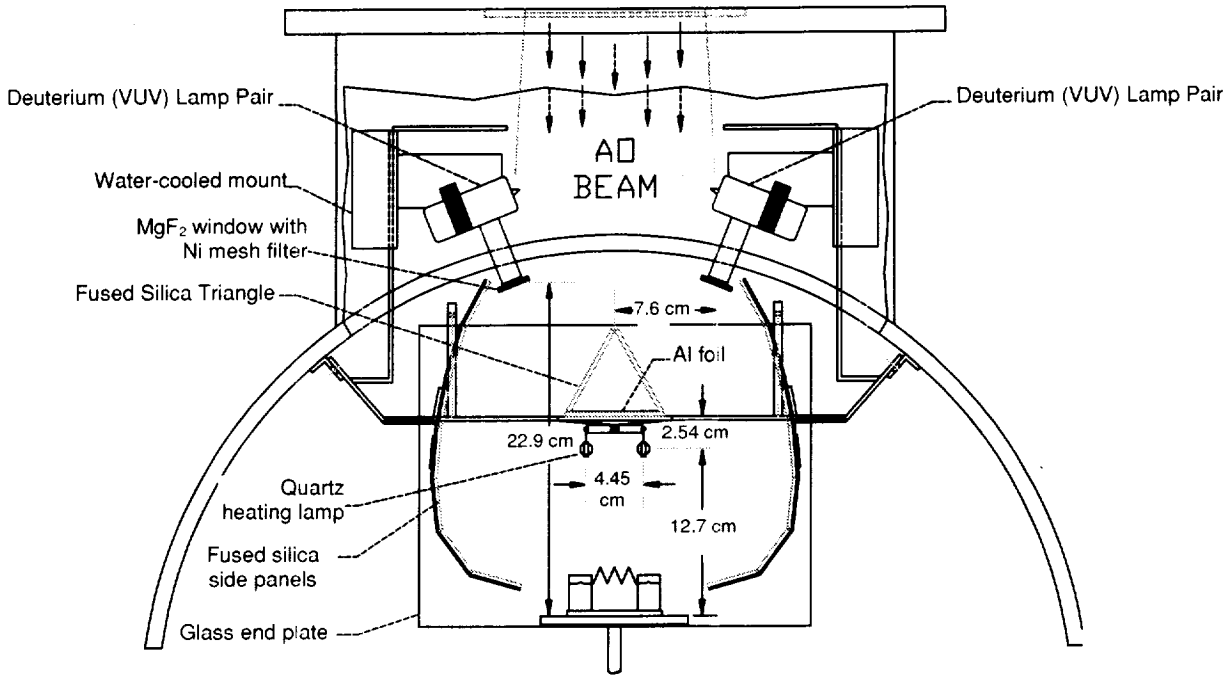

(a)

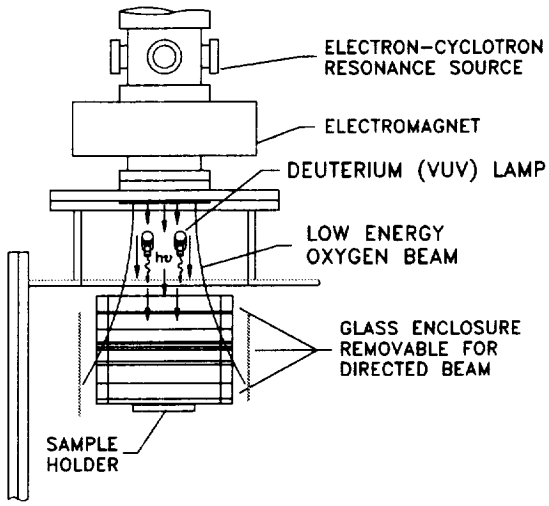

(b)

Figure 6: Arrangement of equipment inside of the atomic oxygen/VUV exposure facility from (a) end view and (b) side view.

2.3 Analysis Methods

2.3.1 Monitoring Contamination at the Sample Site

Contamination witness mirrors labeled Ctm1 and Ctm2 (shown in Figure 4) were measured to determine whether a significant amount of contaminant material was deposited and "fixed" onto the surfaces during VUV and AO exposure. For each compartment, Ctm1 was measured at periodic intervals during testing and Ctm2 was measured prior to exposure and was not re-measured until all exposures to VUV and atomic oxygen were complete. Ctm1 witness mirrors were replaced following the first increment of VUV exposure with new witness mirrors (also referred to as Ctm1) for possible further analysis. The Ctm samples were measured in air for their spectral reflectance between 250 and 2500 nm using a Perkin Elmer Lambda-9 UV-VIS-NIR spectrophotometer equipped

with a 60 mm integrating sphere. Measurements of total and diffuse spectral reflectance were made, and specular reflectance was obtained by subtracting diffuse reflectance from total reflectance at each wavelength. Measurements were made as soon as possible following removal from the vacuum chamber to minimize any potential effects of air bleaching, or reversal of optical property degradation due to air exposure. Spectra were convoluted over the air mass zero solar spectrum to determine integrated values of specular solar reflectance. The standard practices used for measurement and calculation of solar reflectance are described elsewhere [Ref. 11].

2.3.2 Optical Microscopy

All samples were carefully examined with an optical microscope to get an indication of the extent of damage to the samples prior to VUV and after incremental VUV and AO exposures. Optical micrographs between 11.9X-101.4X were obtained using an Olympus SZH stereo-zoom microscope. Images from 4-8 different areas on each welded sample and from 2-4 areas on the planar samples were obtained and sketches were made to show image locations. After incremental environmental exposures, the same areas were imaged to help verify effects of VUV and/or AO exposures. It was difficult to get good quality micrographs, which can only be obtained using the microscope's monocular view, due to the waviness and/or tilt of the samples, and because the samples are second surface reflectors. However, observations were documented based on stereo viewing, which made the front and back surfaces of the samples distinguishable. The welded samples were imaged with the samples propped up on an angle to increase visibility for both weld areas and planar faces. Only the outer weld and approximately the top 2/3 of the planar faces of the welded samples were examined. The inner weld and lower 1/3 planar faces were either at too steep an angle, shadowed, or both, making examination very difficult.

2.3.3 Atomic Force Microscope (AFM) Hardness Determination

Atomic force microscopy was used to measure small changes in the surface hardness due to cross-linking (embrittlement) from VUV, and the amount of removal of the cross-linked surface by AO oxidation. The principle of AFM is to position a sample surface in contact with a microscopic cantilevered probe using a piezo-electric scanner, scan the probe over the sample, and, by reflecting a laser beam off the top of the cantilever, detect and record the exact position of the probe as it moves up and down on the surface. This technique can give <1 Å resolution in the Z direction (normal to the surface). The AFM system moves the sample to a position where the sample is deflecting the cantilever, and while doing this it records the position of the sample and the deflection of the cantilever. For a surface which has infinite hardness, the tip deflection versus sample position (in the Z direction) curve would give a constant steep slope. For a softer sample, as the sample is moved into contact with the tip, there will be both tip deflection and sample indentation, which are recorded. The result is that softer surfaces will have less steep and varying slopes as the probe pushes into the surface. Examples of tip deflection versus sample position slopes for hard (alumina) and soft (Teflon®) samples are given in Figures 7(a) and (b), respectively. By comparing the slopes of the tip deflection versus sample distance curves for elastically deflected surfaces, relative surface hardness can be determined. The absolute hardness value for a surface was not determined, but relative hardness from one surface to another was determined. For the AFM samples, the relative hardness was computed in this manner from the slopes of the tip deflection versus sample distance curves, and is referred to as the "spring constant" of the surface, k'(N/m).

Special AFM samples were made for exposure to VUV and AO with the thermal shield test samples. Sixteen strip samples were made, each with 5 exposure areas per sample. Several exposures are on each AFM strip sample in order to decrease effects such as variations in static charge, moisture, etc. from one sample to another. Cover plates were designed and fabricated with various 2.5 mm circular exposure patterns and were exchanged at specific exposure levels so that each sample had 5 different circular exposure areas on it. The individual strip samples were approximately 4 mm x 22 mm, and each individual exposure area was approximately 2 mm diameter. Because the thermal shield test samples were in a bellows configuration, each surface was at a ≈23.5° incline to the incident VUV and AO flux, therefore the AFM samples were also at a 23.5° incline, and the resulting exposure areas were more elliptical than circular (≈1.8 mm x ≈1 mm). One of the AFM sample assemblies is shown in Figure 3. Samples were designated 1 through 16, and the individual exposure areas were labeled A - E. Approximately half of the 16 AFM samples had duplicate exposures so that results could be verified if necessary. Digital Instruments (DI) conducted surface hardness analyses for seven samples, labeled 1, 2, 4, 7, 9, 11 and 12, and exposure levels for these are provided in section 3.3.1.

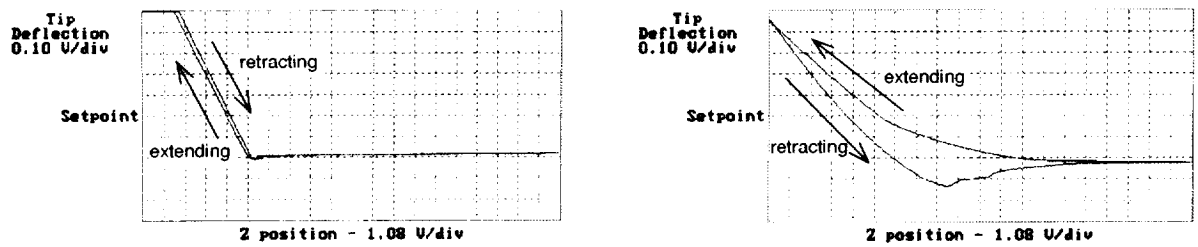

(a) (b)

Figure 7: Tip deflection versus sample position curves for (a) alumina which is a hard surface and produces a steep slope and (b) pristine Teflon® FEP which is a soft surface and produces a less steep slope.

2.3.4 Atomic Force Microscope (AFM) Surface Topography

Surface topography images were obtained at DI for several sample exposure areas using tapping-mode AFM imaging. Images were obtained for 500 nm square scan areas and all images were plotted with identical Z scales and at the same tilt angle.

2.3.5 Light Penetration Photography

Photographs were obtained for samples prior to and following incremental VUV and AO-VUV exposure using back-lighting to a) document the number of pinholes, scratches and cracks in the aluminum prior, during and after VUV and AO-VUV exposure and b) determine whether there was any delamination of the aluminum after VUV and AO-VUV exposure.

Images were obtained by placing samples on a light box with black paper containing an aperture used to block light except below the sample. A Nikon F4 35-mm camera with a 31 mm extension tube and a 200 mm F4 Micro Nikkor lens was mounted on a Polaroid MP-4 chassis approximately 70 cm above the sample site. For all photos, a 4-second exposure was used with an F-stop setting of 32. Kodak T Max ISO 400 film was used. A control sample which was not exposed to VUV or AO was photographed during each photo-session to ensure that the photographic processing would be duplicated.

3. RESULTS AND DISCUSSION

3.1 Monitoring Contamination at the Sample Site

Figure 8 shows a plot of solar specular reflectance of the Ctm1 contamination witness mirrors as a function of VUV exposure. After the first increment of VUV exposure but before the first increment of AO exposure, the Ctm1 witness mirrors for each chamber were removed for possible further analyses and were replaced with new ones, also designated as Ctm1. The plots labeled "inc. 1" are for the first VUV exposure increment. The plots labeled "rem" are for the mirrors which were used for the remainder of the testing after the first VUV exposure increment. Minor fluctuations in the specular reflectance were observed throughout the exposures except in the case of the Group 1 and Group 2 witness mirrors which showed a significant decrease in specular reflectance at approximately 3000 ESH VUV and a restoration of reflectance at approximately 4000 ESH. It is unknown why such degradation occurred at this point and then recovered by the next increment. If contamination was the cause for this reflectance decrease, then any deposited contamination would have been removed from both the witnesses and the samples during the next exposure increment based on the measured restoration of reflectance following the next exposure increment. Atomic oxygen exposure caused slight increases in specular reflectance at each increment probably indicating removal of any VUV facility-produced contaminants.

The contamination witness mirrors that were measured only before and after the entire test, labeled Ctm2, showed a negligible change in specular reflectance. These mirrors were not replaced during the course of VUV and AO-VUV testing. Initial solar specular reflectance was measured to be 0.850, and the maximum change in this value upon exposure to VUV and AO-VUV was ± 0.004 which is within instrument repeatability.

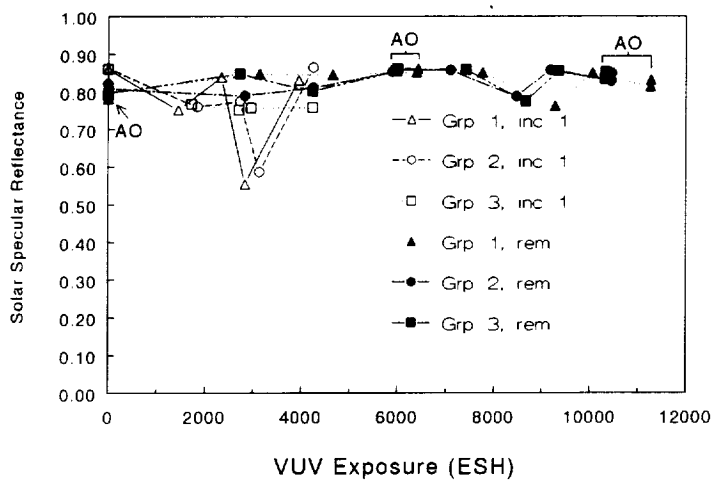

Figure 8: Solar specular reflectance of contamination witness mirrors as a function of VUV exposure.

3.2 Optical Microscopy

During visual examination of the planar and welded samples prior to VUV exposure, it was noticed that the surface of several samples produced colorful sparkled reflections. This can indicate coating failure. Examination of some of these areas using an optical microscope revealed that the coating on these areas was delaminated and spalled. The rainbow sparkles visible to the naked-eye were determined to be curled-up and/or flaked-off patches of film reflecting light in a direction other than that being reflected by the adherent coating. Figures 9 (a) to (d) show representations of the various coating failures observed during optical microscopy examination including cracks, delamination, spalling, and flaking. *Cracks* are defined as breaks in the coating (Fig. 9(a)). *Delamination* is defined as a coating area that has pulled away from the surface (Fig. 9(b)). *Spalling*, is defined as a coating area which is torn and delaminated from the surface and possibly curled or flaked off (Fig. 9(c)). *Flaking* is defined as individual small pieces of coating not adhered to the substrate (Fig 9(d)).

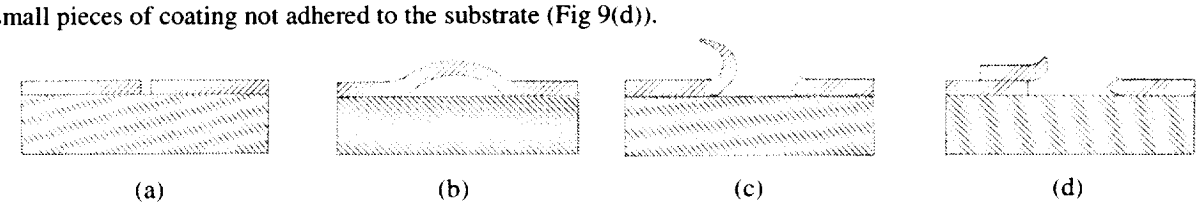

Figure 9: Representations of coating failures observed for the thermal shield samples: (a) cracks, (b) delamination, (c) spalling, and (d) flaking.

3.2.1 Original Coated Samples Prior to VUV Exposure

Optical microscopy examination of SiO_X- and OCLI-coated samples from the first or "original" sample set prior to VUV exposure revealed coating delamination and spalling failures for many samples. A few examples of these coating adhesion problems are shown in Figures 10(a) to (d). A summary of the coating integrity for all of the original coated samples, as indicated by whether or not spalling occurred, is provided in Table 3 (the term "spalled" in this table refers to coating areas that have possibly delaminated, curled-up and/or flaked-off). Detailed optical microscopy examination of the original group of coated samples revealed the following results. For all double-coated samples (SiO_X and OCLI coatings), welded and planar, which had been exposed to RTC there was a serious coating delamination and spalling problem, with the OCLI-coated samples being more severely affected than the SiO_X samples. For the single-coated samples (SiO_X and OCLI coatings), welded and planar, which were exposed to RTC, initial stages of spalling were apparent on approximately one-third to two-thirds of the planar samples, and on both welded samples. All coated samples (SiO_X and OCLI coatings), single and double-coated, welded and planar, which had not been exposed to RTC, often contained cracks in the coatings, but did not have any observable delamination or spalling. Therefore, it was concluded that coating failures occurred upon RTC exposure.

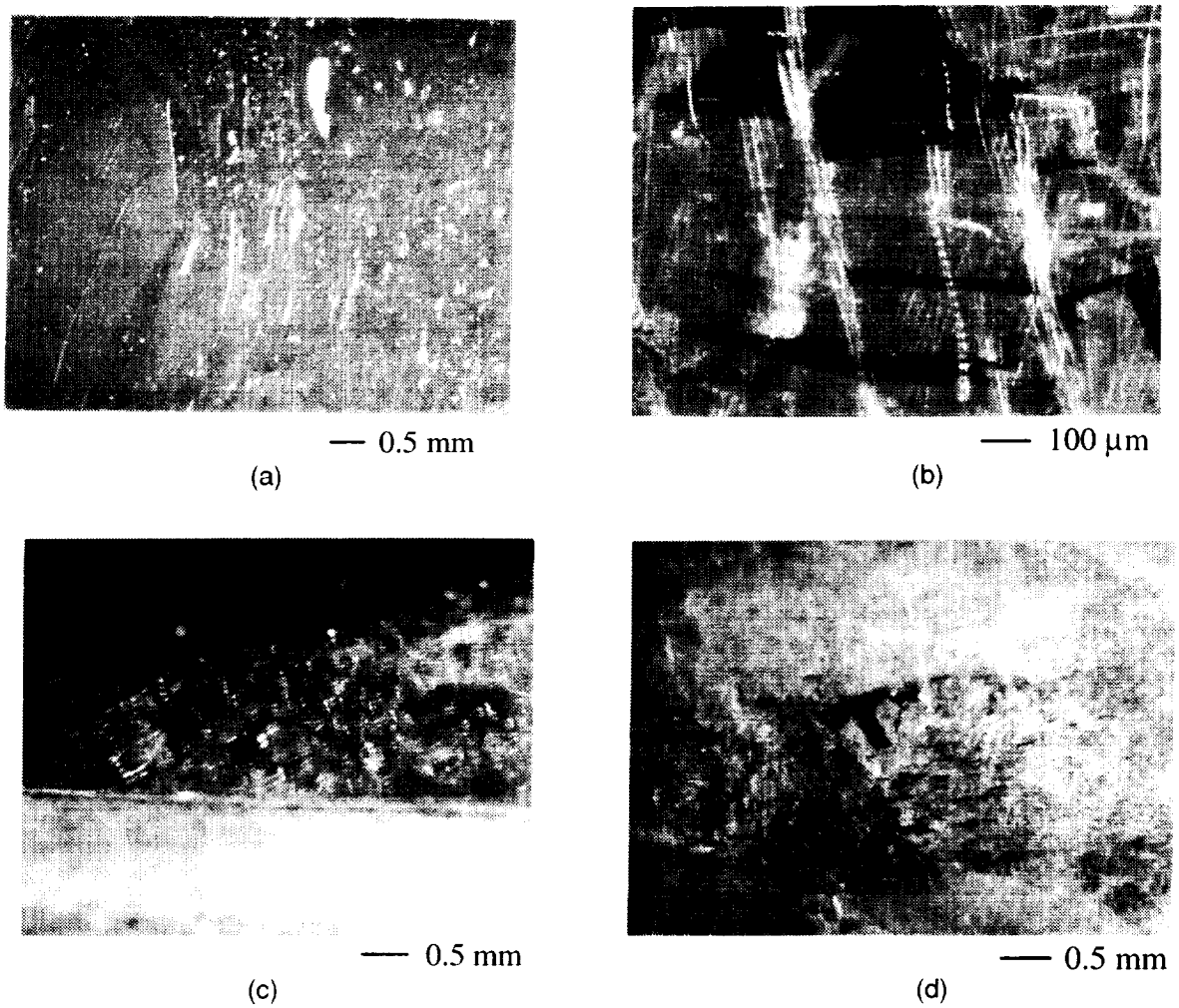

Figure 10: Examples of coating adhesion failures of the original samples prior to VUV exposure for (a) sample ssa-05 where many patches of coating are missing and many coating areas curled up; and (b) sample rra-01, (c) sample rrb-02, and (d) sample rra-08 where dark areas in the micrographs indicate coating areas that are missing.

3.2.2 Original Coated Samples After Initial VUV Exposure

Observations after the first increment of exposure to VUV and AO provided evidence of the very serious nature of spalling as evidenced by the increase in severity of coating spalling and the production of coating particles. Figure 11, a micrograph of sample ssa-05 after initial VUV and AO exposure, typical of the entire sample, shows that the coating is peeling away and flaking off the sample. Rainbow specks were noticed on the fixtures of the Sample Group 3 (OCLI-coated) samples that were concluded to be flakes of OCLI coating on the fixture (see Figure 12(a)). Also, after removal of the sample group from the microscope, there was a piece of OCLI coating (as indicated by a typical blue hue) left on the microscope slide (see Figure 12(b)). There are many possible causes for production of these flakes from the already damaged coatings during the VUV exposure process including: handling (even with very careful handling the samples can vibrate), thermal exposure, collapsing of the welds (which was noticed after the first increment of VUV exposure), and the VUV and AO exposures themselves.

Because of the problem with coating adhesion, a new batch of OCLI-coated samples was prepared in order to improve coating adhesion. These samples were evaluated using optical microscopy and were substituted into the test program. At this stage, the majority of the original OCLI- and SiO_X-coated samples were not tested further. No new SiO_X-coated samples were made, because the OCLI coating was the prime coating candidate.

TABLE 3 - COATING INTEGRITY OF ORIGINAL COATED HST THERMAL SHIELD TEST COUPONS

Sample Description			Rapid Thermal Cycling[a]	# of Samples	# of Samples: Evidence of Spalling
Welded	Single Coating	OCLI	yes	2	2: spalled regions
			no	1	1: no spalling
		SiO_X	yes	-	-
			no	2	2: no spalling
	Double Coating	OCLI	yes	2	2: spalling
			no	1	1: no spalling
		SiO_X	yes	1	1: spalling
			no	-	-
Planar	Single Coating	OCLI	yes	6	1: spalling initiated 1: possible spalling initiated 4: no spalling
			no	2	2: no spalling
		SiO_X	yes	6	1: small sections spalled 3: possible spalling initiated 2: no spalling
			no	-	-
	Double Coating	OCLI	yes	6	6: severe spalling
			no	1	1: no spalling
		SiO_X	yes	3	2: spalling 1: spalling initiated
			no	-	-

[a] 175 thermal cycles between nominal temperature limits of −115 °C to 90 °C although temperature range varied throughout the test.

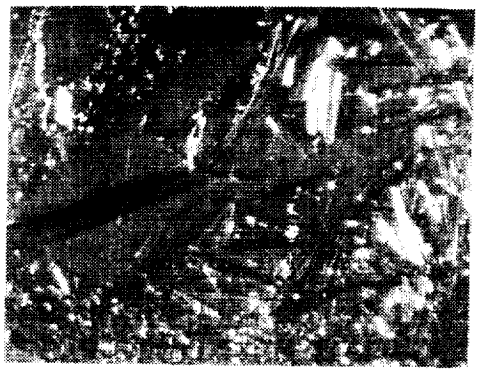

— 0.5 mm

Figure 11: Micrograph of sample ssa-05 showing increased severity of coating spalling following VUV exposure as evidenced by coating flaking off of entire sample.

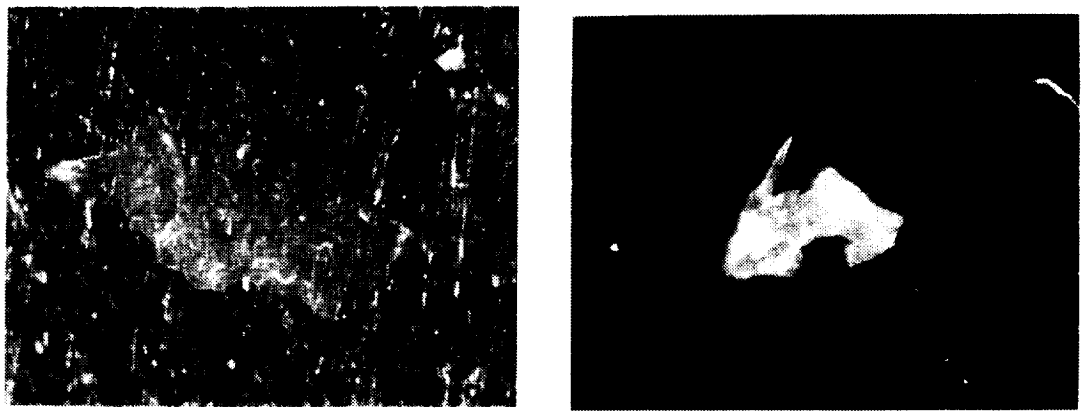

— 100 μm — 100 μm

(a) (b)

Figure 12: Evidence of loose flakes of OCLI coating (a) on sample fixture, and (b) on microscope slide used during sample examinations.

3.2.3 Second Batch of OCLI-Coated Samples Prior to VUV Exposure

Prior to VUV and AO exposure, the second set or "new" OCLI-coated samples, which were not electron irradiated or rapid temperature cycled, were observed to contain occasional coating cracks, particularly in bent areas. Inside the cracks, small coating particles were observed, and there were some areas were the coating appeared to be missing (see Figure 13(a)). Occasionally coating particles from "crack" areas appeared to be loosely attached, and likely to dislodge (see Figure 13(b)). Besides these occasional areas with coating cracks and associated coating debris, there were no observed areas on any of the new OCLI-coated samples with delaminated or spalled coatings.

3.2.4 Second Batch of OCLI-Coated Samples After VUV Exposure

There was no observed coating delamination or spalling of the new OCLI coatings with VUV or AO exposure. The majority of coating particles in the crack areas appeared to remain adherent during VUV and AO exposure, although some particles were found to be missing after exposure (see Figure 14). Also, the outer welds of the samples were observed to have yellowed after the full VUV and AO exposure, possibly due to UV-darkening.

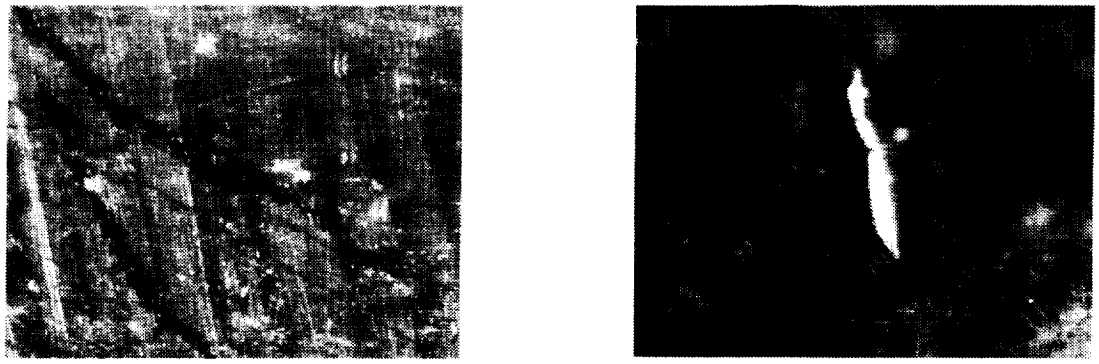

— 100 μm — 100 μm

(a) (b)

Figure 13: New OCLI coated samples prior to VUV exposure showing coating cracks evidenced by (a) dark areas in micrograph of sample rra-101 where coating is missing, and (b) bright area in micrograph of sample rrb-101 where coating from crack site is lifted away from the surface.

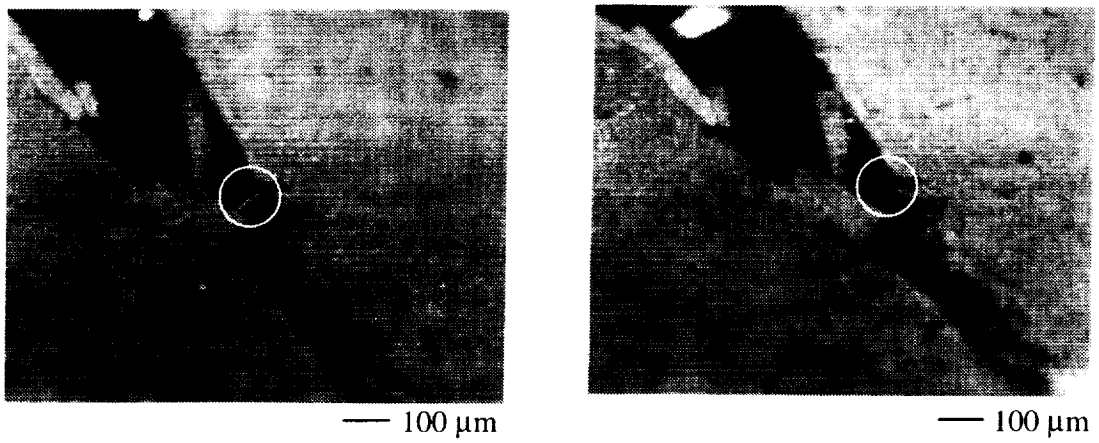

(a) (b)

Figure 14: Crack area in sample rrb-102 (a) prior to and (b) after VUV and AO exposure. Note the small particle in the crack area near the center of micrograph (a) is missing from micrograph (b).

3.2.5 Uncoated Samples Prior to and After VUV/AO Exposure

The uncoated samples had a variety of features prior to VUV exposure including cracks in the aluminum layer, scratches in the Teflon®, and diffuse or hazy appearances. Cracks in the aluminum layer are shown in Figure 15(a) for sample ua-02, and scratches on the Teflon® surface are shown in Figure 15(b) for sample ua-08. The development of hazy patches appeared to increase with increasing VUV and AO exposure. High magnification of these areas shows the haziness to be very fine diffuse spots on the surface of the Teflon®, indicating either surface texturing or contamination. Sample ub-204 had a large hazy patch with a streak through it as seen in Figure 16(a). It is not clear if this hazy patch was present prior to VUV exposure. The hazy patch in the middle upper portion of Figure 16(b) did develop on this sample during environmental exposure. After final VUV and AO exposure, one of the welded samples (ub-03), near an outer weld, had a section that appeared to have been atomic oxygen eroded (see Figure 17). The uneven erosion at the very edge of the weld (likely due to uneven thickness at the edge) resulted in very small sections of Teflon® left almost freestanding, and could result in the production of small Teflon® particles. If produced in space, these fine Teflon® particles would eventually erode away due to atomic oxygen erosion. This particular outer weld was bent over and appears to have received a higher VUV and AO flux than the other welds. Although this was a localized region, a few other welded samples showed evidence of microscopic erosion at the very edge of the outer welds after final VUV and AO exposure.

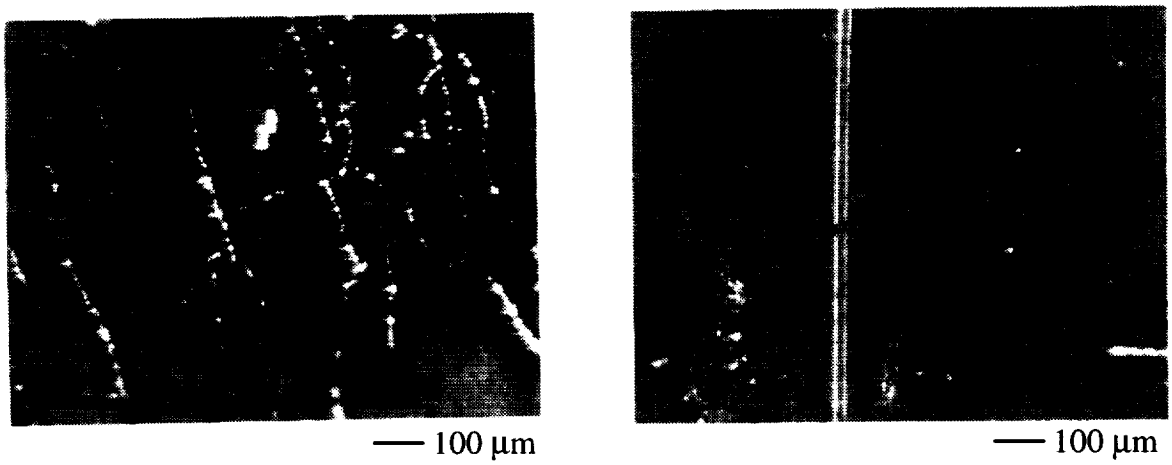

(a) (b)

Figure 15: Examples of surface features observed for uncoated samples: (a) cracks in the aluminum layer of sample ua-02, and (b) scratches in the Teflon® layer of sample ua-08.

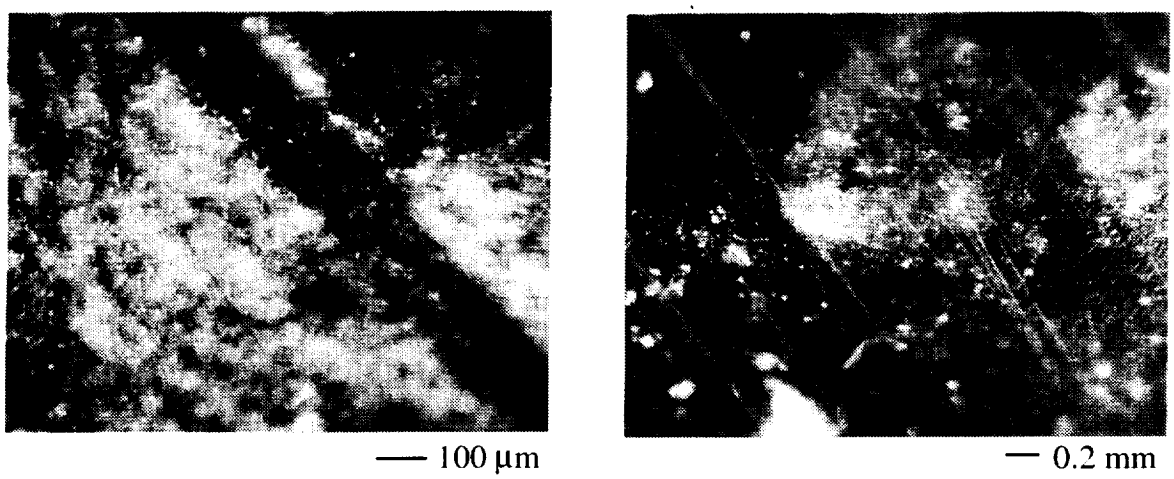

(a) (b)

Figure 16: Examples of hazy area on sample ub-204: (a) hazy patch with a streak through it, may have been present prior to VUV exposure, and (b) hazy patch developed during VUV/AO exposure.

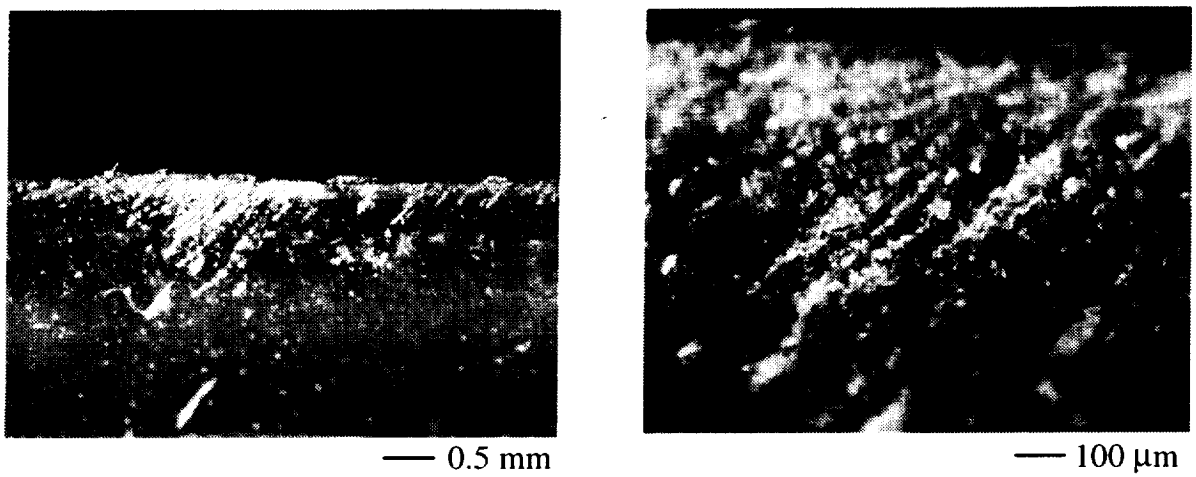

(a) (b)

Figure 17: Atomic oxygen eroded area of an outer weld edge on sample ub-03: (a) small pieces of Teflon® at the top of the weld are left almost free-standing and (b) higher magnification of eroded area showing protective particles lined up in rows.

3.3 Atomic Force Microscopy

3.3.1 AFM Surface Hardness Results

Surface hardness results for the seven AFM samples are given along with their exposure levels in Table 4. Samples 1 and 9 were exposed to increasing levels of VUV, from 0 to 12,573 ESH. These samples were expected to show increasing amounts of hardness due to the VUV-induced cross-linking of FEP Teflon® and resulting embrittlement. As can be seen in Table 4, the hardness for these two samples, as indicated by the spring constant (k') of the surface, did increase from ≈14 N/m for the pristine area to ≈148 N/m for the area exposed to 12,573 ESH of VUV. Plotting spring constant versus weeks of VUV exposure gives a second-order polynomial fit for increase in hardness as a function of VUV exposure resulting in embrittlement (see Figure 18).

TABLE 4 - RELATIVE HARDNESS OF VUV/AO EXPOSED FEP TEFLON® BASED ON AFM TIP DEFLECTION VERSUS POSITION CURVES

Sample	VUV Exposure (ESH)	Atomic Oxygen Exposure (atoms/cm^2)	Atomic Oxygen/VUV Ratio (atoms/(cm^2·ESH))	Spring Constant, k* (N/m^2)
1A	0	0	--	14.4
1B	1012	0	--	21.0
1C	2338	0	--	36.6
1D	3943	0	--	72.0
1E	5741	0	--	82.8
9A	0	0	--	14.0
9B	7468	0	--	123.4
9C	9306	0	--	123.4
9D	10,820	0	--	137.2
9E	12,573	0	--	147.8
7A	0	0	--	13.8
7B	1369	2×10^{19}	1.46×10^{16}	19.2
7C	2966	2×10^{19}	6.74×10^{15}	26.4
7D	4830	4×10^{19}	8.28×10^{15}	37.2
7E	6621	4×10^{19}	6.04×10^{15}	23.4
2A	9.5	4×10^{19}	4.21×10^{18}	13.2
2B	1022	4×10^{19}	3.91×10^{16}	16.8
2C	2348	4×10^{19}	1.70×10^{16}	14.4
2D	3952	4×10^{19}	1.01×10^{16}	19.8
2E	5751	4×10^{19}	6.96×10^{15}	54.0
11A	0	0	--	14.0
11B	7490	5.25×10^{19}	7.01×10^{15}	61.9
11C	9330	5.25×10^{19}	5.63×10^{15}	105.0
11D	10,850	6.5×10^{19}	5.99×10^{15}	43.2
11E	12,603	6.5×10^{19}	5.16×10^{15}	91.4
4A	0	0	--	14.0
4B	33	6.5×10^{19}	1.97×10^{18}	21.9
4C	12,164	6.5×10^{19}	5.34×10^{15}	70.4
4D	12,131	0	--	144.2
4E	12,164	6.5×10^{19}	5.34×10^{15}	70.4
12E	43	1.33×10^{20}	3.09×10^{18}	14.0
12D	7511	1.33×10^{20}	1.77×10^{16}	21.99
12C	9349	1.33×10^{20}	1.42×10^{16}	27.6
12B	10,862	1.33×10^{20}	1.22×10^{16}	50.4
12A	12,616	1.33×10^{20}	1.05×10^{16}	58.1

Results for all of the 7 AFM samples are plotted in Figure 19. Sample 7E was not plotted because there may have been an error in obtaining the data as reported by Digital Instruments. In the legend, AO fluence is in units of atoms/cm^2. As can be seen in the graph, all sample areas which received AO exposure in addition to VUV radiation exposure have lower spring constants and therefore have softer surfaces than the samples which received equivalent VUV exposure with no AO, indicating that the AO is removing some of the surface embrittled layer, as expected. If we examine the results for samples 2 and 7 (with AO fluence of 2-4 x 10^{19} atoms/cm^2) as compared to sample 1 which had approximately equivalent exposure to VUV but was not exposed to AO, it can be seen that an AO exposure of 2 x 10^{19} atoms/cm^2 (sample 7) only partially removes the embrittled layer formed by cross-linking upon exposure to 1369 and 2966 ESH VUV. Whereas, results from sample 2 indicate that an AO fluence of 4 x 10^{19} atoms/cm^2 did remove the embrittled layer for up to 2348 ESH of VUV exposure.

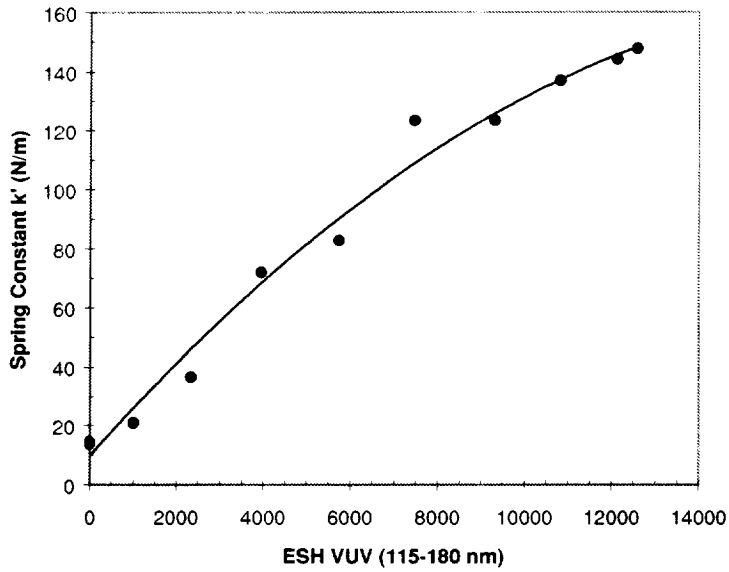

Figure 18: Increase in surface hardness of Teflon® FEP is indicated by an increase in the spring constant with VUV exposure. Second order polynomial curve fit is shown.

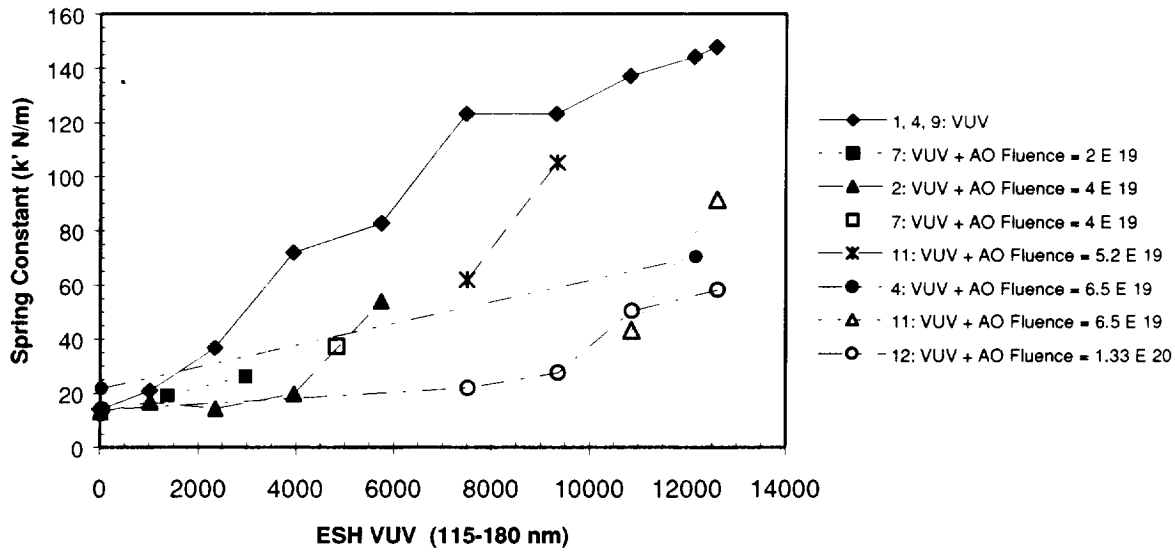

Figure 19: Spring constant versus VUV exposure for AFM samples. Based on higher values of spring constant for samples exposed only to VUV and lower values for samples exposed to both VUV and AO, it is evident that AO exposure removes some of the surface embrittled layer caused by VUV exposure.

As described earlier, the anticipated ratio of AO fluence to VUV equivalent sun hours in the HST environment is $\approx 4 \times 10^{15}$ atoms/(cm^2·ESH). It was desired to expose certain samples to this ratio in order to determine the degree to which AO would remove the VUV-embrittled layer on the HST thermal shields. Several sample areas were meant to receive this AO/VUV ratio; however, the samples that received the closest to this ratio were sample areas 11E, (AO/VUV ratio of 5.16×10^{15} atoms/(cm^2·ESH)) and sample areas 4C and 4E (AO/VUV ratio of 5.34×10^{15} atoms/(cm^2·ESH)). All other sample areas received even higher AO/VUV ratios. The significance of the AO-VUV ratio is that any value greater than 4×10^{15} atoms/(cm^2·ESH) indicates that the sample received a greater amount of AO erosion relative to the depth of VUV embrittlement than the anticipated HST equivalent space exposure increments. Despite the excess AO exposure, the VUV-hardened surface layer of Teflon® on samples 11E, 4C and 4E (with the AO/VUV ratio closest to that expected in the HST environment) was not removed. Therefore, it is concluded based on the results from the AFM samples, that for anticipated HST thermal shield AO/VUV exposure levels, AO will remove some of the VUV-embrittled surface layer, but will not completely remove it, and a surface embrittled layer will build up on the Teflon® HST solar array thermal shields that could form cracks.

3.3.2 AFM Topography Images

Atomic force microscopy topographical images of sample 7A (pristine), 4D (no AO, high ESH VUV), 12E (low ESH VUV and high AO fluence), and 12A (high ESH VUV and high AO fluence) are shown in Figure 20.

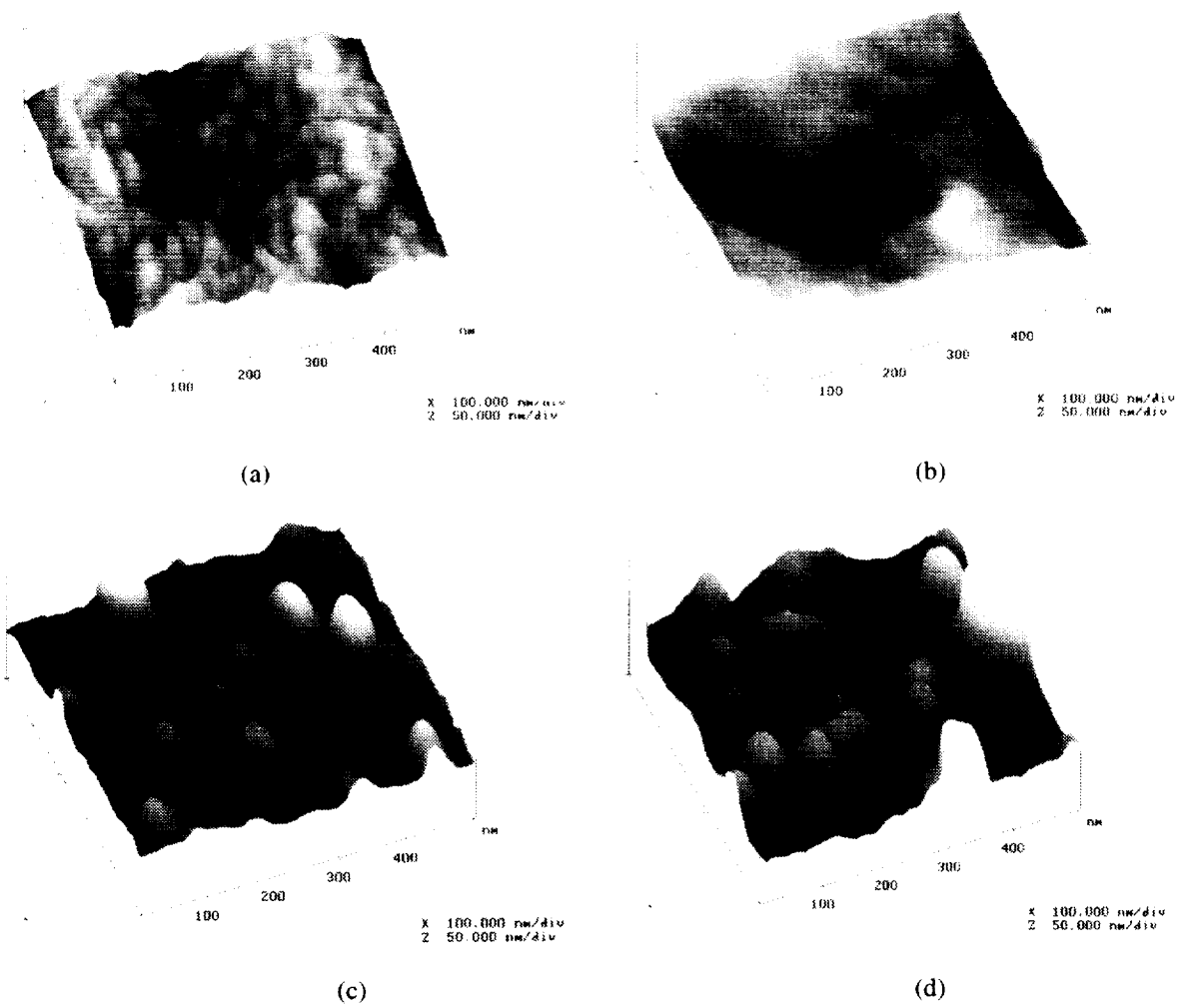

Figure 20: AFM surface topography images: (a) sample 7A (pristine), (b) sample 4D (12,131 ESH VUV), (c) sample 12E (43 ESH VUV and AO fluence of 1.33×10^{20} atoms/cm^2), and (d) sample 12A (12,616 ESH VUV and AO fluence of 1.33×10^{20} atoms/cm^2).

The pristine surface image for sample 7A (Figure 20(a)) shows a series of small linear mounds. Sample 4D (Figure 20(b)), exposed to 12,131 ESH of VUV exposure, shows a definite difference in the surface morphology. The VUV-exposed surface appears to be microscopically smoother, and the linear mounds are no longer present. Sample 12E (Figure 20(c)) which was exposed to a minimal amount of VUV (43 ESH) and an AO fluence in excess of that expected for 5 years in the HST environment (1.33×10^{20} atoms/cm^2), has the appearance of small rounded cone structures typical of atomic oxygen exposure. In between the cones, the surface is smooth with only a hint of the linear mounds. Sample 12A (Figure 20(d)) which was exposed to 12,616 ESH VUV and an AO fluence of 1.33×10^{20} atoms/cm^2, appears similar to sample 12E, with slightly larger cone structures.

3.4 Light Penetration Photography

Evaluation of the light penetration photographs indicated no significant changes in the number or appearance of pinholes, scratches and cracks in the aluminum layer of the samples. A few samples showed a slight increase in the number of pinholes and scratches probably attributed to handling rather than to environmental exposure. Comparison of photographs taken before and after VUV and AO-VUV exposure did not show delamination of the aluminum for any of the samples. Figure 21(a) and (b) shows light penetration photographs for sample ua-02 prior to and after VUV and AO-VUV exposure. The fact that this sample had previously been exposed to RTC and was bend-tested, one would expect that it would be most susceptible to aluminum delamination. However, no increase in the number of pinholes, scratches or cracks was observed as can be seen in Figure 21.

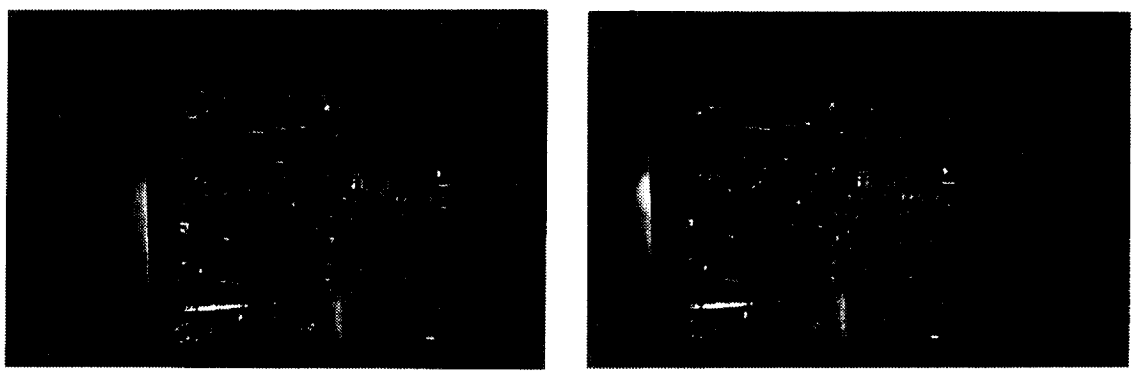

(a) (b)

Figure 21: Light penetration photograph of sample ua-02 (a) before and (b) after VUV and AO-VUV exposure.

4. SUMMARY AND CONCLUSIONS

Candidate HST solar array bi-stem thermal shield materials were ground tested to estimate their durability for up to five years in the HST environment. Samples of these candidate materials, aluminized FEP Teflon® with and without AO- and AO/UV-protective coatings, were exposed to VUV and to AO combined with VUV at operational temperatures of 105 °C, for uncoated and SiO_X-coated samples, and 135 °C, for OCLI coated samples, in a test that simulated up to approximately five years on HST. Some of these samples were previously exposed to 0.5 Mrads of 1 MeV electron radiation and 175 rapid thermal cycles nominally between –115 °C and 90 °C although temperature range varied due to equipment malfunctions. Optical microscopy, light penetration photography, and AFM were used to characterize the samples. Molecular contamination of the sample chambers during the VUV and AO-VUV exposures, determined by examining reflectance changes on witness mirrors, was assessed to be negligible for the overall test duration.

The original group of samples of aluminized FEP Teflon® with SiO_X and OCLI coatings showed serious coating adhesion, delamination, and spalling problems that were worse for double-coated areas. It was determined that the coating delamination was induced during RTC exposure. Samples that had not been RTC-exposed were not delaminated and spalled. The delamination problem was found to worsen with exposure to VUV and AO and is likely to be due to heating to operational temperatures during these test and/or necessary handling. Newer OCLI-coated samples were found to have pieces of coating missing from coating crack sites, but, in general, were not delaminated and spalled like the originally supplied OCLI-coated samples. It should be noted, however, that the

newer OCLI-coated samples were not exposed to RTC. Exposure of the newer OCLI-coated samples to VUV and AO at operational temperatures did not cause coating delamination. The uncoated aluminized Teflon® samples were found to have minimal degradation with five-year equivalent VUV and AO exposure at operational temperatures and prior exposure to electron radiation and rapid thermal cycling. Minor atomic oxygen-induced erosion at the very edge of the outer welds of a few samples was observed. The uncoated samples also developed some hazy areas which were attributed to erosion texturing or localized contamination. AFM hardness analysis of the uncoated aluminized FEP samples tested in this study revealed increasing VUV-induced embrittlement of uncoated Teflon® with increasing VUV exposure. AO exposure did not completely remove this embrittled surface layer despite the fact that all samples received a higher AO fluence to VUV exposure ratio than expected for the HST environment.

Due to the extreme problem with the coated samples producing flakes of glass-like particles associated with coating spalling upon thermal cycling, and the minor degradation observed with VUV and AO exposure to the uncoated samples, uncoated aluminized Teflon® FEP was determined to be the best of the three materials for the HST solar array bi-stem boom thermal shields, and this material was used on replacement HST solar arrays that were installed in December 1993, and which will be replaced in early 2002.

Based on the AFM hardness data, for anticipated AO and VUV exposure levels in the HST environment, an embrittled surface layer is expected to build up on the uncoated aluminized FEP Teflon® solar array bi-stem thermal. Because bulk embrittlement has occurred on other HST-exposed FEP materials due to the overall environmental exposure conditions, embrittlement of the thermal shields is expected to be more severe than the AFM samples would predict based on their exposure to only VUV and AO. The embrittled layer is not expected to produce flakes of material that would interfere with or degrade performance of the HST optics during operation. However, FEP embrittlement from the overall HST environment exposure could cause formation of cracks and potential particulate contamination due to stresses on the thermal shields upon retraction during future servicing missions.

6. REFERENCES

1. Banks, B.A., et al., "Atomic Oxygen Interactions with FEP Teflon® and Silicones on LDEF," NASA Conference Publication 3134, Part 2, p. 801, June 1991.

2. Brinza, D.E. et al., "Vacuum Ultraviolet (VUV) Radiation-Induced Degradation of Fluorinated Ethylene Propylene (FEP) Teflon® Aboard the Long Duration Exposure Facility (LDEF)," NASA Conference Publication 3134, Part 2, p. 817, June 1991.

3. Townsend, J.A., Hansen, P.A., Dever, J.A., de Groh, K.K., Banks, B.A., Wang, L., He, C., "Hubble Space Telescope metallized Teflon® FEP thermal control materials: on-orbit degradation and post-retrieval analysis," High Performance Polymers, Vol. 11, No. 1, March 1999, p. 98.

4. Photograph courtesy of Public Relations, British Aerospace Space Systems Limited, Bristol, UK, Photograph Number 87519/9, March 1993.

5. K.K. de Groh, J.R. Gaier, R.L. Hall, M.P. Espe, D.R. Cato, J.K. Sutter and D.A. Scheiman, "Insights into the damage mechanism of Teflon® FEP from the Hubble Space Telescope," High Performance Polymers, Vol. 12, No. 1, pp. 83-104, 2000.

6. Dever, J.A., de Groh, K.K., Messer, R.K., McClendon, M.W., Viens, M., Wang, L., Gummow, J., "Mechanical properties of Teflon® FEP retrieved from the Hubble Space Telescope," High Performance Polymers, Volume 13, No. 3, September 2001, pp. S373-S390.

7. de Groh, K.K., Dever, J.A., Sutter, J.K., Gaier, J.R., Gummow, J.D., Schieman, D.A., He, C., "Thermal contributions to the degradation of Teflon® FEP on the Hubble Space Telescope," High Performance Polymers, Volume 13, No. 3, September 2001, pp. S401-S420.

8. Dever, J.A., Pietromica, A.J., Stueber, T.J., Sechkar, E.A., Messer, R.K., "Simulated Space Vacuum Ultraviolet (VUV) Exposure Testing for Polymer Films," AIAA-2001-1054, American Institute of Aeronautics and Astronautics, January 2001.

9. Banks, B.A., "The use of fluoropolymers in space applications," Chapter 4 in Modern Fluoropolymers, edited by John Schiers, John Wiley & Sons, Chichester, UK, 1997.

10. Rutledge, S.K., Banks, B.A., "A Technique for Synergistic Atomic Oxygen and Vacuum Ultraviolet Radiation Durability Evaluation of Materials for use in LEO," NASA Technical Memorandum 107230, April 1996.

11. ASTM E 903-82, "Standard Test Method for Solar Absorptance, Reflectance, and Transmittance of Materials Using Integrating Spheres," Annual Book of ASTM Standards, Vol. 12.02, American Society of Testing and Materials, 1982 (edited and re-approved 1992).

REPORT DOCUMENTATION PAGE

Form Approved
OMB No. 0704-0188

Public reporting burden for this collection of information is estimated to average 1 hour per response, including the time for reviewing instructions, searching existing data sources, gathering and maintaining the data needed, and completing and reviewing the collection of information. Send comments regarding this burden estimate or any other aspect of this collection of information, including suggestions for reducing this burden, to Washington Headquarters Services, Directorate for Information Operations and Reports, 1215 Jefferson Davis Highway, Suite 1204, Arlington, VA 22202-4302, and to the Office of Management and Budget, Paperwork Reduction Project (0704-0188), Washington, DC 20503.

1. AGENCY USE ONLY (*Leave blank*)

2. REPORT DATE
February 2002

3. REPORT TYPE AND DATES COVERED
Technical Memorandum

4. TITLE AND SUBTITLE
Vacuum Ultraviolet Radiation and Atomic Oxygen Durability Evaluation of HST Bi-Stem Thermal Shield Materials

5. FUNDING NUMBERS
WU–755–1A–13–00

6. AUTHOR(S)
Joyce Dever and Kim K. de Groh

7. PERFORMING ORGANIZATION NAME(S) AND ADDRESS(ES)
National Aeronautics and Space Administration
John H. Glenn Research Center at Lewis Field
Cleveland, Ohio 44135–3191

8. PERFORMING ORGANIZATION REPORT NUMBER
E–13185

9. SPONSORING/MONITORING AGENCY NAME(S) AND ADDRESS(ES)
National Aeronautics and Space Administration
Washington, DC 20546–0001

10. SPONSORING/MONITORING AGENCY REPORT NUMBER
NASA TM—2002-211364

11. SUPPLEMENTARY NOTES
Responsible person, Joyce Dever, organization code 5480, 216–433–6294.

12a. DISTRIBUTION/AVAILABILITY STATEMENT
Unclassified - Unlimited
Subject Categories: 18 and 27 Distribution: Nonstandard
Available electronically at http://gltrs.grc.nasa.gov/GLTRS
This publication is available from the NASA Center for AeroSpace Information, 301–621–0390.

12b. DISTRIBUTION CODE

13. ABSTRACT ***(Maximum 200 words)***

Bellows-type thermal shields were used on the bi-stems of replacement solar arrays installed on the Hubble Space Telescope (HST) during the first HST servicing mission (SM1) in December 1993. These thermal shields helped reduce the problem of thermal gradient-induced jitter observed with the original HST solar arrays during orbital thermal cycling and have been in use on HST for eight years. This paper describes ground testing of the candidate solar array bi-stem thermal shield materials including backside aluminized Teflon® FEP (fluorinated ethylene propylene) with and without atomic oxygen (AO) and ultraviolet radiation protective surface coatings for durability to AO and combined AO and vacuum ultraviolet (VUV) radiation. NASA Glenn Research Center (GRC) conducted VUV and AO exposures of samples of candidate thermal shield materials at HST operational temperatures and pre- and post-exposure analyses as part of an overall program coordinated by NASA Goddard Space Flight Center (GSFC) to determine the on-orbit durability of these materials. Coating adhesion problems were observed for samples having the AO- and combined AO/UV-protective coatings. Coating delamination occurred with rapid thermal cycling testing which simulated orbital thermal cycling. This lack of adhesion caused production of coating flakes from the material that would have posed a serious risk to HST optics if the coated materials were used for the bi-stem thermal shields. No serious degradation was observed for the uncoated aluminized Teflon® as evaluated by optical microscopy, although atomic force microscopy (AFM) microhardness testing revealed that an embrittled surface layer formed on the uncoated Teflon® surface due to vacuum ultraviolet radiation exposure. This embrittled layer was not completely removed by AO erosion. No cracks or particle flakes were produced for the embrittled uncoated material upon exposure to VUV and AO at operational temperatures to an equivalent exposure of approximately five years in the HST environment. Uncoated aluminized FEP Teflon® was determined to be the most appropriate thermal shield material and was used on the bi-stems of replacement solar arrays installed on HST during SM1 in December 1993. The SM1-installed solar arrays are scheduled to be replaced during HST's fourth servicing mission (SM3B) in early 2002.

14. SUBJECT TERMS
Far ultraviolet radiation; Oxygen atoms; Teflon®; Hubble Space Telescope

15. NUMBER OF PAGES
29

16. PRICE CODE

17. SECURITY CLASSIFICATION OF REPORT	18. SECURITY CLASSIFICATION OF THIS PAGE	19. SECURITY CLASSIFICATION OF ABSTRACT	20. LIMITATION OF ABSTRACT
Unclassified	Unclassified	Unclassified	